NASA/TM—2000-209948 AIAA 2000–1961

Acoustics and Thrust of Separate-Flow Exhaust Nozzles With Mixing Devices for High-Bypass-Ratio Engines

Naseem H. Saiyed
Glenn Research Center, Cleveland, Ohio

Kevin L. Mikkelsen
Aero Systems Engineering, St. Paul, Minnesota

James E. Bridges
Glenn Research Center, Cleveland, Ohio

June 2000

The NASA STI Program Office . . . in Profile

Since its founding, NASA has been dedicated to the advancement of aeronautics and space science. The NASA Scientific and Technical Information (STI) Program Office plays a key part in helping NASA maintain this important role.

The NASA STI Program Office is operated by Langley Research Center, the Lead Center for NASA's scientific and technical information. The NASA STI Program Office provides access to the NASA STI Database, the largest collection of aeronautical and space science STI in the world. The Program Office is also NASA's institutional mechanism for disseminating the results of its research and development activities. These results are published by NASA in the NASA STI Report Series, which includes the following report types:

- TECHNICAL PUBLICATION. Reports of completed research or a major significant phase of research that present the results of NASA programs and include extensive data or theoretical analysis. Includes compilations of significant scientific and technical data and information deemed to be of continuing reference value. NASA's counterpart of peer-reviewed formal professional papers but has less stringent limitations on manuscript length and extent of graphic presentations.
- TECHNICAL MEMORANDUM. Scientific and technical findings that are preliminary or of specialized interest, e.g., quick release reports, working papers, and bibliographies that contain minimal annotation. Does not contain extensive analysis.
- CONTRACTOR REPORT. Scientific and technical findings by NASA-sponsored contractors and grantees.
- CONFERENCE PUBLICATION. Collected papers from scientific and technical conferences, symposia, seminars, or other meetings sponsored or cosponsored by NASA.
- SPECIAL PUBLICATION. Scientific, technical, or historical information from NASA programs, projects, and missions, often concerned with subjects having substantial public interest.
- TECHNICAL TRANSLATION. English-language translations of foreign scientific and technical material pertinent to NASA's mission.

Specialized services that complement the STI Program Office's diverse offerings include creating custom thesauri, building customized data bases, organizing and publishing research results . . . even providing videos.

For more information about the NASA STI Program Office, see the following:

- Access the NASA STI Program Home Page at ***http://www.sti.nasa.gov***
- E-mail your question via the Internet to help@sti.nasa.gov
- Fax your question to the NASA Access Help Desk at (301) 621-0134
- Telephone the NASA Access Help Desk at (301) 621-0390
- Write to:
  NASA Access Help Desk
  NASA Center for AeroSpace Information
  7121 Standard Drive
  Hanover, MD 21076

NASA/TM—2000-209948 AIAA 2000–1961

Acoustics and Thrust of Separate-Flow Exhaust Nozzles With Mixing Devices for High-Bypass-Ratio Engines

Naseem H. Saiyed
Glenn Research Center, Cleveland, Ohio

Kevin L. Mikkelsen
Aero Systems Engineering, St. Paul, Minnesota

James E. Bridges
Glenn Research Center, Cleveland, Ohio

Prepared for the
Sixth Aeroacoustics Conference and Exhibit
cosponsored by the American Institute of Aeronautics and Astronautics
and Confederation of European Aerospace Societies
Lahaina, Hawaii, June 12–14, 2000

National Aeronautics and
Space Administration

Glenn Research Center

June 2000

Available from

NASA Center for Aerospace Information
7121 Standard Drive
Hanover, MD 21076
Price Code: A03

National Technical Information Service
5285 Port Royal Road
Springfield, VA 22100
Price Code: A03

ACOUSTICS AND THRUST OF SEPARATE-FLOW EXHAUST NOZZLES WITH MIXING DEVICES FOR HIGH-BYPASS-RATIO ENGINES

Naseem H. Saiyed
National Aeronautics and Space Administration
Glenn Research Center
Cleveland, Ohio 44135

Kevin L. Mikkelsen
Aero Systems Engineering
358 Fillmore Avenue East
St. Paul, Minnesota 55107

and

James E. Bridges
National Aeronautics and Space Administration
Glenn Research Center
Cleveland, Ohio 44135

SUMMARY

The NASA Glenn Research Center recently completed an experimental study to reduce the jet noise from modern turbofan engines. The study concentrated on exhaust nozzle designs for high-bypass-ratio engines. These designs modified the core and fan nozzles individually and simultaneously. Several designs provided an ideal jet noise reduction of over 2.5 EPNdB for the effective perceived noise level (EPNL) metric.

Noise data, after correcting for takeoff thrust losses, indicated over a 2.0-EPNdB reduction for nine designs. Individually modifying the fan nozzle did not provide attractive EPNL reductions. Designs in which only the core nozzle was modified provided greater EPNL reductions. Designs in which core and fan nozzles were modified simultaneously provided the greatest EPNL reduction. The best nozzle design had a 2.7-EPNdB reduction (corrected for takeoff thrust loss) with a 0.06-point cruise thrust loss. This design simultaneously employed chevrons on the core and fan nozzles.

In comparison with chevrons, tabs appeared to be an inefficient method for reducing jet noise. Data trends indicate that the sum of the thrust losses from individually modifying core and fan nozzles did not generally equal the thrust loss from modifying them simultaneously. Flow blockage from tabs did not scale directly with cruise thrust loss and the interaction between fan flow and the core nozzle seemed to strongly affect noise and cruise performance. Finally, the nozzle configuration candidates for full-scale engine demonstrations are identified.

INTRODUCTION

The impetus for this study was the increasingly stringent noise regulations designed to protect the communities around airports from aircraft noise pollution. Jet exhaust is one of the dominant noise sources from modern turbofan engines (ref. 1), its dominance dramatically increasing with throttle push. These engines use two nozzles (fig. 1) to separately exhaust flow from the core and fan, hence the name separate-flow nozzles (SFN's). Mixing these two flows into a single flow prior to exhausting provides a thrust benefit relative to two separate flows (ref. 2). However, integration factors associated with mixing the two flows (e.g., extra nacelle weight, drag and thrust reverser complexity) negate the thrust benefits for high-bypass-ratio engines.

The NASA Glenn Research Center (GRC) recently completed an exhaustive experimental study to evaluate the jet noise reduction from new SFN designs. This study, the Separate Flow Nozzle Test (SFNT), was part of

NASA's Advanced Subsonic Technology program and was a team effort between GRC, NASA Langley (LaRC), Pratt & Whitney (PW), United Technologies Research Corporation (UTRC), Boeing, General Electric (GE), Allison (AEC), and Aero Systems Engineering (ASE). The data from the study were collected on far-field acoustics, plume Schlieren images, exhaust plume pressures and temperatures, plume infrared signatures, jet noise source locations, and thrust performance.

Many of the new SFN designs attempted to reduce the fully expanded jet velocity by mixing (a) core flow with fan flow only, (b) fan flow with ambient flow only, or (c), (a) and (b) simultaneously. Based on the type of flow mixing attempted, these designs fell into two broad categories: tabs and chevrons. Very aggressive mixing characterized the tabs and very gentle, the chevrons. Remaining SFN designs attempted to shield the hot core jet using a scarfed fan and offset fan nozzles. The SFNT study tested 54 SFN configurations[1,2] including various alterations of SFN designs within each category (tabs and chevrons).

Several of the 54 SFN configurations provided an "ideal" jet noise reduction of over 2.5 EPNdB on the basis of the EPNL metric (ref. 3). This assumed that the thrust performance remained identical between the baseline SFN and new SFN's. This report considers the actual takeoff thrust performance in evaluating the EPNL benefits (reductions). It also recommends particular SFN's that may be good candidates for further development via static engine tests and flight tests for possible implementation in commercial service.

OBJECTIVES

In this report, the ideal EPNL values were corrected for takeoff thrust performance. The corrections were made for several SFN configurations in which tab and chevron designs and their individual and simultaneous use on core and fan nozzles were varied.

The cruise thrust data were examined to determine the effect of specific SFN design parameters on cruise thrust performance. To allow greater variation in their specific designs, a few more SFN configurations were tested for cruise thrust data than were tested for takeoff thrust data.

ACOUSTIC TESTS AT NASA GLENN RESEARCH CENTER

Acoustic data were collected on 54 SFN configurations. These tests were conducted at a typical high-bypass-ratio cycle (fig. 2). The model spectra were scaled up by a factor of 8. Ideal EPNL values were calculated for level flyover at a 1500-ft altitude with a simulated flight speed of Mach 0.28. No ground corrections were applied because only relative EPNL's were desired. These EPNL's, spectra, and other details of the SFNT are presented in Janardan[1] and in Low.[2] The 54 SFN's were reduced to 14 SFN's for thrust performance tests. This selection was based on the EPNL metric and geometric variations among the configurations.

THRUST PERFORMANCE TESTS AT AERO SYSTEMS ENGINEERING

Figure 2 also shows the takeoff and cruise cycle points for the thrust performance tests. Unlike the acoustic tests, the thrust performance tests were not run hot because SFN's utilize separate nozzles for core and fan flows, which do not mix within a mixing chamber. Consequently, the temperature of nonmixed flows has no impact on the nozzle thrust coefficient C_{Tr}:

$$C_{Tr} = \frac{F_g^d}{F_g^i} \tag{1}$$

where F_g^d is the measured gross thrust with a force balance and F_g^i is the ideal gross thrust from

$$F_g^i = \dot{m}_c v_{i,c} + \dot{m}_f v_{i,f} \tag{2}$$

[1]Janardan, B.A., et al.: AST Critical Propulsion and Noise Reduction Technologies for Future Commercial Subsonic Engines: Separate-Flow Exhaust System Noise Reduction Concept Evaluation. NASA/CR—2000-210039, to be published.

[2]Low, J.K.C.; Schweiger, P.S.; and Premo, J.W.: Advanced Subsonic Technology (AST) Separate-Flow High-Bypass Ratio Nozzle Noise Reduction Program Test Report. NASA/CR—2000-210040, to be published.

where $\dot{m}_c$ and $\dot{m}_f$ are core and fan flow rates, respectively, and $v_{i,c}$ and $v_{i,f}$ are core and fan ideally expanded jet velocities, respectively. Therefore, C_{Tr} values from cold thrust performance tests would be identical to C_{Tr} values from hot thrust performance tests. Also, cold performance tests provide a stable model free of thermal expansion and and heat transfer between the ducts. FluiDyne quotes the accuracy to be ±0.25 points for absolute values of C_{Tr} at simulated flight.

The takeoff thrust performance data were acquired statically (M 0.0) and at simulated flight (M 0.28). Static data were acquired for SFN configurations in which only the core nozzle was modified. In these configurations simulated flight was not necessary because fan flow isolated the core nozzle from ambient flow. Simulated flight data were acquired for SFN configurations in which the fan nozzle was modified (either individually or simultaneously with the core nozzle).

The cruise thrust performance data were acquired at M 0.8 for all SFN configurations.

HARDWARE

The 14 SFN's selected from acoustic tests employed tabs and chevrons. Following is a brief description of their major characteristics with specific details given in Janardan[3] and Low.[4] Figure 3 shows a test configuration of the baseline SFN (also known as 3BB) and its cross section at the core exit plane. The SFN hardware designation is $3\text{-}X_a\text{-}Y_b$, where 3 is the model number, X is the core nozzle designation, Y is the fan nozzle designation, and subscripts a and b refer to the number of tabs or chevrons on each nozzle. For example,[5] $3T_{48}C_{24}$ signifies that model 3 has a core nozzle with 48 tabs and a fan nozzle with 24 chevrons. All nozzles were convergent.

Tabs: Core Nozzle

Delta tabs were used to produce strong streamwise vortices to aggressively mix the core flow with the fan flow. Some tabs protruded into the core flow and some into the fan flow. The tab protrusion angle was 30° with respect to the core streamlines (ref. 4). Some tabs did not protrude into either flow; that is, they remained neutral with a protrusion angle of 0°. Figure 4 shows two core nozzle tab configurations ($3T_{24}B$ and $3T_{48}B$). The six tabs protruding into the core flow for $3T_{24}B$ blocked 2.9 percent of the core geometric throat area. The 12 tabs protruding into the core flow for $3T_{48}B$ blocked 1.45 percent of the core geometric throat area.

Tabs: Fan Nozzle

To aggressively mix the fan flow with the ambient flow, delta tabs were used to produce strong streamwise vortices. Some tabs protruded into the fan flow and some into the ambient flow. The tab protrusion angle was 30° with respect to the fan streamlines (ref. 4). Some tabs did not protrude into either flow but remained neutral with a protrusion angle of 0°. Figure 5 shows tabs on fan nozzle configuration $3BT_{48}$. The 12 tabs protruding into the fan flow blocked about 2 percent of the fan geometric throat area.

Chevrons: Core Nozzle

Chevrons are serrations on the nozzle exit plane for creating streamwise vortices, albeit much more gently than the delta tabs do. Figure 6 shows 3 configurations with 12 chevrons each ($3C_{12}B$, $3I_{12}B$, and $3A_{12}B$). The $3C_{12}B$ configuration has simple serrations on the nozzle exit plane; these remain parallel with core streamlines. Chevrons from the $3I_{12}B$ configuration protruded into the core flow only about one displacement thickness of the core boundary layer. They were inclined about 3° with respect to core streamlines, a very gradual inclination. Chevrons from the $3A_{12}B$ configuration protruded into both the core flow and the fan flow. They were also gradually inclined about 3° with respect to core streamlines.

[3]Janardan, B.A., et al.: AST Critical Propulsion and Noise Reduction Technologies for Future Commercial Subsonic Engines: Separate-Flow Exhaust System Noise Reduction Concept Evaluation. NASA/CR—2000-210039, to be published.
[4]Low, J.K.C.; Schweiger, P.S.; and Premo, J.W.: Advanced Subsonic Technology (AST) Separate-Flow High-Bypass Ratio Nozzle Noise Reduction Program Test Report. NASA/CR—2000-210040, to be published.
[5]B, baseline; C., chevron; T, tab; I, inward; A, alternating.

Chevrons: Fan Nozzle

Figure 7 shows fan chevron configuration $3BC_{24}$. The 24 chevrons were simple serrations on the nozzle exit plane and remained parallel with fan streamlines. No other chevron design was tried.

Core and Fan Nozzles: Simultaneously

The hardware in the configurations described thus far modified the core and fan nozzles individually. Both nozzles were modified simultaneously for six tests. Figure 8 shows these six combinations: $3T_{24}T_{48}$, $3T_{48}T_{48}$, $3T_{48}C_{24}$, $3I_{12}C_{24}$, $3A_{12}C_{24}$, and $3T_{24}C_{24}$.

FACILITIES

The acoustic tests were conducted in the NASA Glenn Aeroacoustic Propulsion Laboratory (AAPL), a 65-ft-radius geodesic dome (fig. 9). Castner (ref. 5) and Cooper (ref. 6) give additional details about the dome. Since Cooper's report, the concrete floor of the AAPL was covered with 2-ft-high acoustic wedges to upgrade the facility to fully anechoic status. Located inside and at the center 10 ft above the concrete floor is the jet exit rig, which simulates hot engine flows and to which the test articles are attached. A 53-in.-diameter duct (free jet) surrounds the rig and provides the air to simulate flight on the rig and on the test article. The free jet and the jet exit rig comprise the Nozzle Acoustic Test Rig (NATR). A set of 1/4-in. microphones (26 total) located 10 ft above the concrete floor surround the rig from 40° (forward arc) to 165° (aft arc) in 5° increments. The microphones are located at a nominal radius of 50 ft from the test article.

The performance tests were conducted at ASE's FluiDyne Aerotest Laboratory. Static and simulated flight test setups are shown in figures 10(a) and (b), respectively.

EXPERIMENTAL RESULTS

This section presents the results of correcting the ideal acoustic performance of 14 SFN's (based on the EPNL metric) for takeoff thrust performance and the effects of SFN design parameters on cruise performance. Suggestions are made regarding the further development of candidate SFN's for possible implementation into service.

Thrust-Corrected Effective Perceived Noise Levels

The actual gross thrust at GRC $F^a_{g,GRC}$ during hot acoustic tests is now determined. First, the ideal gross thrust at ASE $F^i_{g,ASE}$ is corrected to standard sea level (SSL) pressure $\left(F^i_{g,ASE}\right)_{SSL}$. The behavior of C_{Tr} as a function of $\left(F^i_{g,ASE}\right)_{SSL}$ is found next for each of the 14 SFN's by curve fitting C_{Tr} and $\left(F^i_{g,ASE}\right)_{SSL}$ data:

$$C_{Tr} = f\left(F^i_{g,ASE}\right)_{SSL} \tag{3}$$

Then, the ideal gross thrust at GRC during hot acoustic tests $F^i_{g,GRC}$ is corrected to SSL pressure $\left(F^i_{g,GRC}\right)_{SSL}$ and equation (3) is evaluated at $\left(F^i_{g,GRC}\right)_{SSL}$:

$$C_{Tr} = f\left(F^i_{g,GRC}\right)_{SSL} \tag{4}$$

Values of C_{Tr} from equation (4) could be used to determine actual gross thrust at GRC during hot acoustic tests corrected to SSL pressure $\left(F^a_{g,GRC}\right)_{SSL}$. Determining $F^a_{g,GRC}$ in terms of $F^i_{g,GRC}$ cancels the SSL pressure correction factor. Therefore, the value of $F^a_{g,GRC}$ is calculated from

$$F^a_{g,GRC} = C_{Tr} F^i_{g,GRC} \tag{5}$$

Day-to-day changes in ambient conditions slightly alter $F^i_{g,GRC}$. All EPNL data are corrected by normalizing $F^i_{g,GRC}$ against a reference thrust of 100 lb_f, which assures that variations in EPNL are from SFN designs and not from variations in $F^i_{g,GRC}$.

The normalized EPNL's are plotted against the fully mixed jet velocity V_{mix} normalized with the ambient speed of sound C_{amb}:

$$Z = \frac{V_{mix}}{C_{amb}} \tag{6}$$

where V_{mix} is calculated from

$$V_{mix} = \frac{F^a_{g,GRC}}{\dot{m}_c + \dot{m}_f} \tag{7}$$

Takeoff Effective Perceived Noise Level Benefits

Acoustic tests of the 3BB SFN were repeated several times during the SFNT. Plotting these data as EPNL's versus Z collapsed the entire 3BB data set;[6,7] therefore, these data are represented by a curve fit rather than by symbols to avoid data clutter. The EPNL benefits are reductions in EPNL values relative to 3BB. Also, the value of 1.07 for Z, representing the average growth takeoff thrust, was selected for evaluating the EPNL benefits.

Tabs: core nozzle.—Figure 11 presents an EPNL plot for two SFN's with core tabs ($3T_{24}B$ and $3T_{48}B$). The EPNL benefits appear to be a function of both tab size and thrust. The $3T_{48}B$ EPNL benefits appear to become constant at 1.9 EPNdB beyond 1.05 Z. The $3T_{24}B$ benefits, however, appear to continually increase with thrust, providing about 2.5 EPNdB at 1.07 Z. EPNL benefits seem to increase with tab size at high thrust values, and the trend is reversed at very low thrust values.

Chevrons: core nozzle.—Figure 12 presents EPNL plots for two core chevrons and shows an increase again in EPNL benefit with thrust. The $3I_{12}B$ SFN provided a benefit of 2.1 EPNdB, which is significantly better than that obtained from $3C_{12}B$ at 1.2 EPNdB. The obvious difference between these two configurations is that the $3I_{12}B$ SFN penetrated the boundary layer and $3C_{12}B$ SFN remained parallel with the core streamlines. It seems that some boundary layer penetration, however small, is needed for greater noise reduction.

Tabs and chevrons: fan nozzle.—The fan nozzle boattail angle was 14°. This high value was needed to assure that Glenn's baseline acoustic data could be compared with similar data planned for NASA Langley's Jet Noise Laboratory. Also, this value was a compromise among various nacelles because tests could not be repeated for particular nacelles from each aerospace company.

Figure 13 shows the fan cowl pressure coefficient c_p at Mach 0.8 calculated from

$$c_p = \frac{P_{s,surface} - P_{s,tunnel}}{q} \tag{8}$$

where $P_{s,surface}$ is the surface static pressure, $P_{s,tunnel}$ is the tunnel static pressure, and q is the tunnel dynamic pressure. Except for the last port, all static ports were flush with the surface. The nozzle lip was too thin to flush mount the last static port. Instead, tubing was attached to the nozzle surface, its opening flush with the nozzle base. The flow rapidly expands around the fan shoulder. Such high expansion is reasonable given that the afterbody was not tapered in these tests (refs. 9 to 11). There was no clear evidence of shocks and flow separation, and the expansion appears to recover smoothly. Slight over compression is seen in the last half of the nozzle.

Figure 14 presents an EPNL plot for fan chevrons ($3BC_{24}$) and fan tabs ($3BT_{48}$). Apparently, the $3BC_{24}$ SFN was a little louder than 3BB, achieving an EPNL benefit of only –0.2 EPNdB. The $3BT_{48}$ SFN, however, provided a benefit of about 1.1 EPNdB with respect to 3BB SFN at 1.07 Z and a benefit of about –1.0 EPNdB at low thrust (Z = 0.85). At low thrust, the 48 tabs simply could not entrain air to slow the jet exhaust enough to cause a significant reduction in low-frequency jet noise; in fact, the attempt to do so created high-frequency noise.

---

[6]Janardan, B.A., et al.: AST Critical Propulsion and Noise Reduction Technologies for Future Commercial Subsonic Engines: Separate-Flow Exhaust System Noise Reduction Concept Evaluation. NASA/CR—2000-210039, to be published.

[7]Low, John K.C.; Schweiger, Paul S.; and Premo, John W.: Advanced Subsonic Technology (AST) Separate-Flow High-Bypass Ratio Nozzle Noise Reduction Program Test Report. NASA/CR—2000-210040, to be published.

Core chevrons with fan chevrons: simultaneously.—The EPNL benefits from individually modified core nozzles and fan nozzles were presented in the previous sections. The results of modifying these nozzles simultaneously are now presented. Figure 15 compares the EPNL's from an SFN simultaneously using chevrons on core and fan nozzles ($3I_{12}C_{24}$) with 3BB. A benefit of about 2.7 EPNdB is seen at 1.07 Z and seems to remain constant beyond high thrusts. This figure also compares $3I_{12}C_{24}$ data with that for $3I_{12}B$ and $3BC_{24}$. Adding chevrons to the fan nozzle increased the EPNL benefit of $3I_{12}B$ SFN from 2.1 to 2.7 EPNdB.

Core tabs with fan tabs: simultaneously.—Figure 16 compares the EPNL's from an SFN simultaneously using tabs on the core and fan nozzles ($3T_{24}T_{48}$) with 3BB. The EPNL benefit of about 2.4 EPNdB is seen at growth takeoff thrust and seems to continually increase with thrust. This figure also compares $3T_{24}T_{48}$ data with that from $3T_{24}B$ and $3BT_{48}$. Adding tabs to the fan nozzle did not provide any EPNL benefits at high thrust, but doing so at low thrust ($Z = 0.85$) decreased the EPNL benefit from –1.0 to –1.4 EPNdB.

Cruise Performance

All cruise data were taken at Mach 0.8. Changes in C_{Tr} values relative to 3BB are shown as ΔC_{Tr}. The units of ΔC_{Tr} are in points with 1 point representing a 0.01 change in the C_{Tr} value. For example, the ΔC_{Tr} for a nozzle with a C_{Tr} value of 0.98 is 2.0 points relative to an ideal nozzle with a C_{Tr} value of 1.0. In this section, the effects of SFN design parameters on ΔC_{Tr} are shown.

Tabs: core nozzle.—Figure 17 shows the effect of two tab designs ($3T_{24}B$ and $3T_{48}B$). The $3T_{24}B$ SFN had a 0.99-point loss in C_{Tr} and $3T_{48}B$ SFN had a 0.77-point loss. The $3T_{24}B$ SFN blocked 2.9 percent of the core flow and $3T_{48}B$ SFN blocked 1.45 percent. Reducing the blockage by one-half did not reduce the C_{Tr} loss by one-half probably because of additional losses from expansion.

Chevrons: core nozzle.—Figure 18 shows the effect of three chevron designs ($3C_{12}B$, $3I_{12}B$, and $3A_{12}B$). The C_{Tr} loss for $3C_{12}B$ SFN was 0.55 point with the loss for $3I_{12}B$ and $3A_{12}B$ nearly identical at 0.32 and 0.34 point, respectively. The $3C_{12}B$ SFN was less efficient than the other two core chevron designs even though it did not obstruct the flow.

Tabs and chevrons: fan nozzle.—Figure 19 compares a tab fan nozzle ($3BT_{48}$) and a chevron fan nozzle ($3BC_{24}$). Tabs had a 0.57-point loss and chevrons, a 0.18-point loss.

Core tabs with fan tabs: simultaneously.—Figure 20 shows the impact of adding fan tabs with two core tabs ($3T_{24}T_{48}$ and $3T_{48}T_{48}$). The $3T_{24}B$ SFN had a 0.99-point C_{Tr} loss. Adding the fan nozzle with 48 tabs with its 0.57-point loss ($3BT_{48}$) did not result in a 1.56-point loss for $3T_{24}T_{48}$. Instead, the C_{Tr} loss was 1.14 points for $3T_{24}T_{48}$. The $3T_{48}B$ SFN had a 0.77-point C_{Tr} loss. If fan flow and core flow were independent of each other, the total loss should have been 1.34 points for $3T_{48}T_{48}$; instead, the total loss was 1.1 points.

Core tabs with fan chevrons: simultaneously.—Figure 21 shows the impact of adding fan chevrons with two core tabs ($3T_{24}C_{24}$ and $3T_{48}C_{24}$). The $3T_{24}B$ SFN had a 0.99-point loss and $3BC_{24}$, a 0.18-point loss. Adding the fan nozzle with 24 chevrons to $3T_{24}B$ did not yield a 1.17-point loss. Instead, the total C_{Tr} loss for $3T_{24}C_{24}$ was 0.43 point. Similarly, the C_{Tr} loss with $3T_{48}C_{24}$ was 0.51 point, not 0.95 point.

Core chevrons with fan chevrons: simultaneously.—Figure 22 shows the impact of adding fan chevrons with two core chevrons ($3I_{12}C_{24}$ and $3A_{12}C_{24}$). The $3I_{12}B$ SFN had a 0.32-point loss and $3BC_{24}$, a 0.18-point loss. Together they totaled 0.5 point, but the loss for $3I_{12}C_{24}$ SFN was a paltry 0.06 point.

The $3A_{12}B$ SFN had a 0.34-point loss. Adding fan chevrons to this SFN should have produced a 0.52-point loss. Indeed, the total thrust loss was 0.49 point. Only in this configuration did linearly summing the C_{Tr} losses from modifying individual flows equal C_{Tr} losses from modifying them simultaneously. Some of the summing differences can be attributed to repeatability. However, the general trend shows that performance losses from simultaneous modifications were less than the sum of individual modifications.

Separate-Flow-Nozzle Candidates for Further Development

Jet noise reduction without thrust loss is a very challenging requirement. The constraints of a particular application dictate the jet noise reduction needed and the tolerable thrust loss. For this generic document, these limits are set as (a) a maximum cruise thrust loss of 0.5 point and (b) a minimum EPNL reduction of 2.5 EPNdB. Although no cruise thrust loss is desirable, SFN's with C_{Tr} losses above 0.5 point are likely to be extremely unfavorable. Jet noise reductions less than 2.5 EPNdB are likely to have a much smaller effect on the airplane total EPNL reductions. A particular application will dictate these limits; however, 0.5-point and 2.5-EPNdB limits provide a starting place.

Figure 23 shows C_{Tr} losses and EPNL benefits from 13 SFN's relative to the SFN 14, the 3BB. The thrust-corrected EPNL benefits (actual EPNL benefits) are shown only for the first eight SFN's ($3C_{12}B$ to $3T_{24}T_{48}$). Takeoff thrust data on remaining configurations was not acquired. This figure also shows the ideal EPNL benefits for all configurations. It appears that cruise thrust losses of up to 1.2 points do not significantly affect the actual EPNL benefits. The ideal EPNL benefits are shown for the remaining five SFN's ($3A_{12}B$ to $3T_{48}C_{24}$) because takeoff thrust data were not taken for these configurations. Regardless of the configuration or cruise thrust loss, the EPNL benefits did not change much. This means that $3I_{12}C_{24}$, $3T_{24}C_{24}$, and $3A_{12}C_{24}$ can easily meet the 0.5-point and 2.5-EPNdB limits. The $3A_{12}B$ and $3T_{48}C_{24}$ SFN's border on meeting the limits, so these five should be considered as candidates for further development and verification via static engine tests and flight tests. Table I summarizes the noise benefits and thrust penalties for all configurations.

SUMMARY

NASA Glenn recently completed an extensive experimental study to reduce jet noise. The study concentrated on exhaust nozzle designs for high-bypass-ratio turbofan engines with separate-flow nozzles. A total of 54 SFN's were tested by modifying the core nozzle alone, the fan nozzle alone, or both nozzles simultaneously. Increasing the number of core nozzle tabs ($3T_{24}B$ and $3T_{48}B$) seemed to limit the EPNL benefits to a constant beyond 1.02. Tests with two core chevrons ($3I_{12}B$ and $3C_{12}B$) showed that when the chevrons penetrated the core boundary layer ($3I_{12}B$), they provided greater noise reduction than without penetration. Their EPNL benefits seemed to remain constant beyond 1.0 Z. Chevrons on the fan nozzle ($3BC_{24}$) were not as effective as they were on the core nozzle ($3C_{12}B$). Tabs on the fan nozzle ($3BT_{48}$) also were not as effective as they were on the core nozzle. Modifying the core and fan nozzles simultaneously provided a greater EPNL benefit than modifying either nozzle individually. Specifically, the $3I_{12}C_{24}$ and $3T_{24}T_{48}$ SFN's provided 2.7- and 2.5-EPNdB benefits, respectively.

Reducing the tab blockage from core tabs by one-half did not reduce the C_{Tr} loss by one-half ($3T_{24}B$ and $3T_{48}B$). The design of the Chevron effected its particular loss ($3C_{12}B$, $3I_{12}B$ and $3A_{12}B$). The C_{Tr} losses with chevrons on the fan nozzle were less than C_{Tr} losses with tabs on the fan nozzle. The C_{Tr} losses from modifying the core and fan nozzles simultaneously were not equal to the sum of C_{Tr} losses from modifying them individually. Specifically, the $3I_{12}C_{24}$ and $3T_{24}T_{48}$ SFN's had 0.06- and 1.14-point C_{Tr} losses, respectively. Table I summarizes the EPNL benefits and the cruise thrust losses.

A metric was selected to find the suitable SFN's for further development and verification via static engine tests and flight tests. The metric was the maximum C_{Tr} loss of 0.5 point and the minimum EPNL benefit of 2.5 EPNdB. Five SFN's that achieved the metric and therefore should be considered for further development are $3I_{12}C_{24}$, $3T_{24}C_{24}$, $3A_{12}C_{24}$, $3A_{12}B$, and $3T_{48}C_{24}$.

REFERENCES

1. Groeneweg, J.F.; and Rice, E.J.: Aircraft Turbofan Noise. J. Turbomach., vol. 109, 1987, pp. 130–141.
2. Kerrebrock, J.L.: Aircraft Engines and Gas Turbines. Second edition, MIT Press, Cambridge, MA, 1992.
3. Smith, M.J.T.: Aircraft Noise. Cambridge University Press, Cambridge, MA, 1989.
4. Zaman, K.B.M.Q.; Reeder, M.F.; and Samimy, M.: Control of an Axisymmetric Jet Using Vortex Generators. Phys. Fluids, vol. 6, no. 2, 1994.
5. Castner, R.S.: The Nozzle Acoustic Test Rig: An Acoustic and Aerodynamic Free-Jet Facility. NASA TM–106495 (AIAA Paper 94–2565), 1994.
6. Cooper, B.A.: A Large Hemi-Anechoic Enclosure for Community-Compatible Aeroacoustic Testing of Aircraft Propulsion Systems. NASA TM–106015, 1993.
7. Blaha, B.J.; Chamberlin, R.; and Bober, L.J.: Boundary Layer Thickness Effect on Boattail Drag. NASA TMX–73443, 1976.
8. Chamberlin, R.: Flight Investigation of 24° Boattail Nozzle Drag at Varying Subsonic Flight Conditions. NASA TMX–2626, 1972.
9. Wing, D.J.: Afterbody/Nozzle Pressure Distributions of a Twin-Tail Twin-Engine Fighter With Axisymmetric Nozzles at Mach Numbers from 0.6 to 1.2. NASA TP–3509, 1995.
10. Wing, D.J.: Performance Characteristics of Two Multiaxis Thrust-Vectoring Nozzles at Mach Numbers up to 1.28. NASA TP–3313, 1993.
11. Burley, J.R., II; and Berrier, B.L.: Investigation of Installation Effects of Single-Engine Convergent-Divergent Nozzles. NASA TP–2078, 1982.

TABLE I.—EFFECTIVE PERCEIVED NOISE LEVEL BENEFITS AND CRUISE LOSSES

Separate-flow nozzle configuration	Effective perceived noise level benefit, ENPNdB		Cruise thrust loss, ΔC_{T_r}, points
	Ideal	Actual	
3BB	0	0	0
$3BC_{24}$	−0.16	−0.18	.18
$3C_{12}B$	1.38	1.36	.55
$3I_{12}B$	2.29	2.18	.32
$3I_{12}C_{24}$	2.82	2.71	.06
$3T_{24}B$	2.73	2.37	.99
$3T4_{48}$	2.29	2.09	.77
$3BT_{48}$	1.22	1.05	.57
$3T_{24}T_{48}$	2.56	2.04	1.14
$3T_{48}T_{48}$	2.77		1.1
$3A_{12}B$	2.59		.34
$3A_{12}C_{24}$	3.52		.49
$3T_{24}C_{24}$	3.16		.43
$3T_{48}C_{24}$	2.58		.51

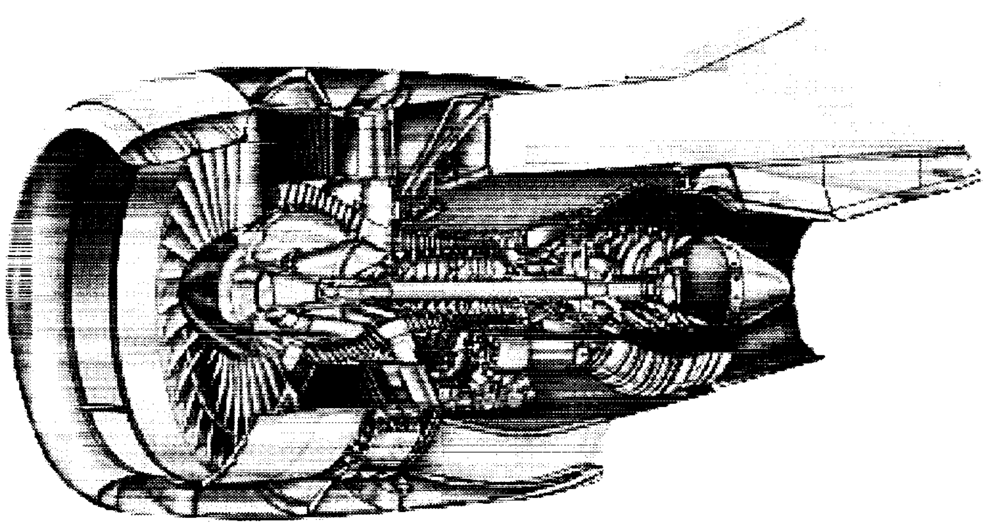

Figure 1.—Typical high-bypass-ratio, separate flow engine.

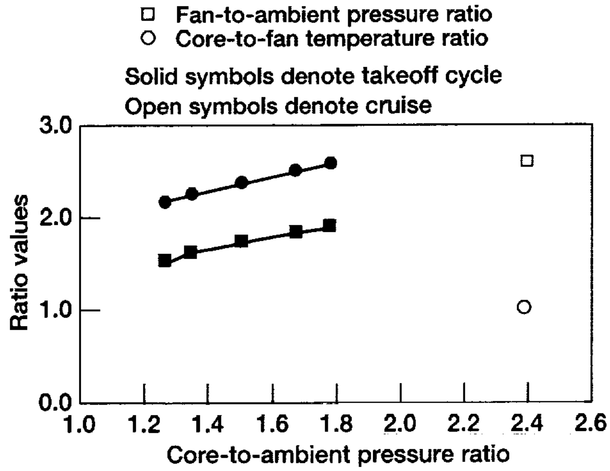

Figure 2.—Cycle points for acoustic and thrust performance tests.

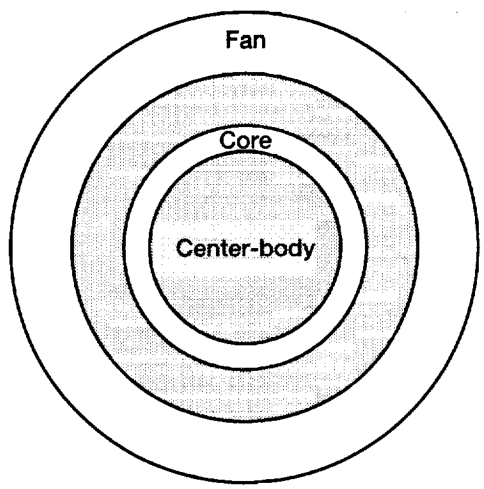

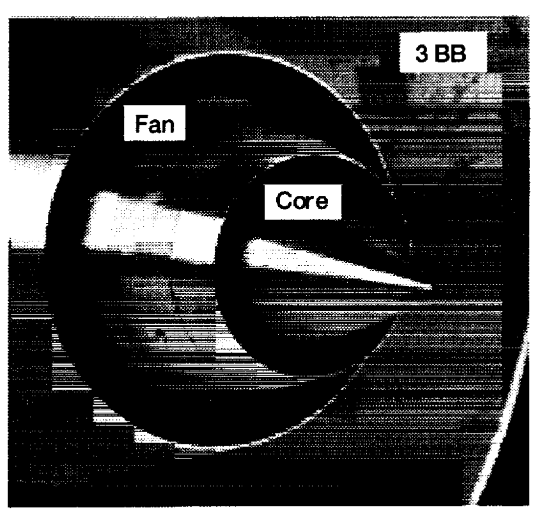

Figure 3.—Typical high-bypass-ratio, separate-flow nozzles. Area of fan, A_{fan}, 28.9 in.^{2} Area of core, A_{core}, 10.5 in.^{2}

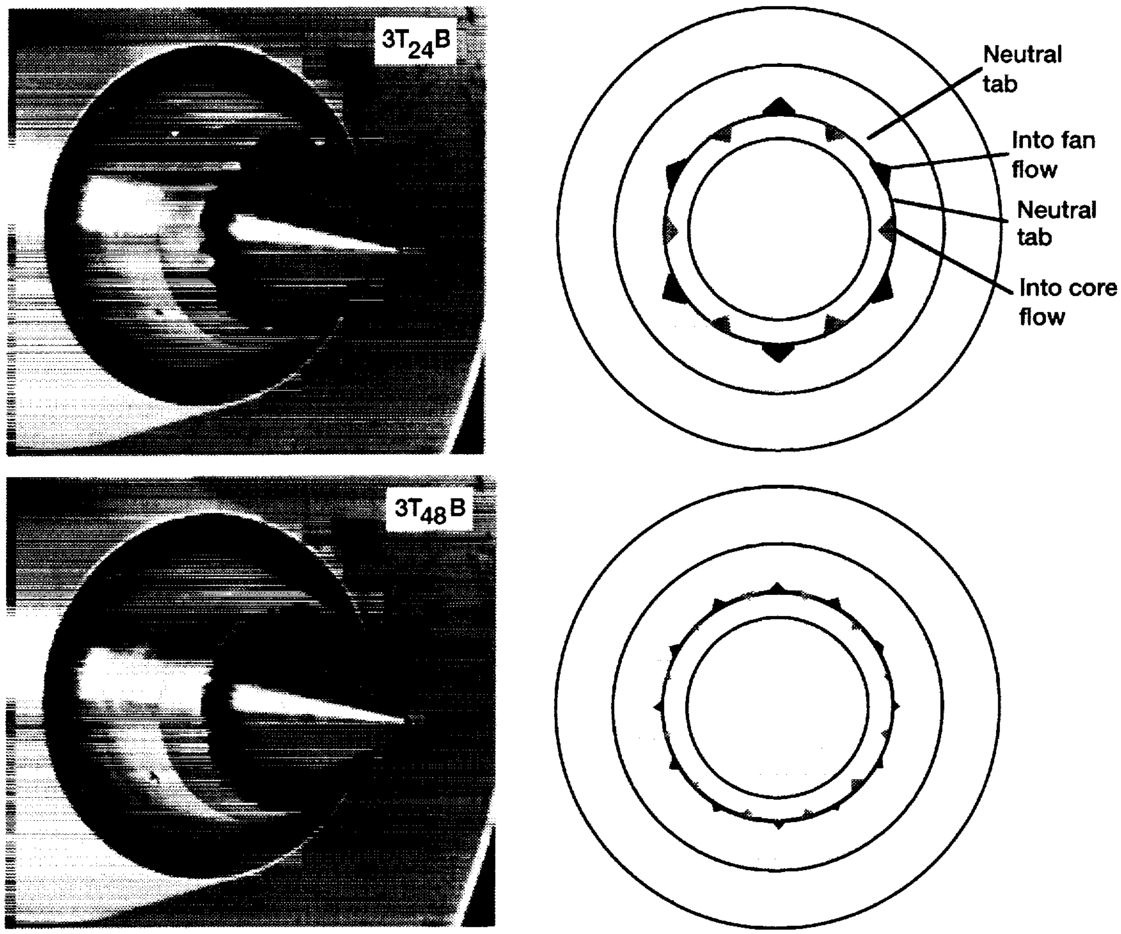

Figure 4.—Tabs on core nozzle only.

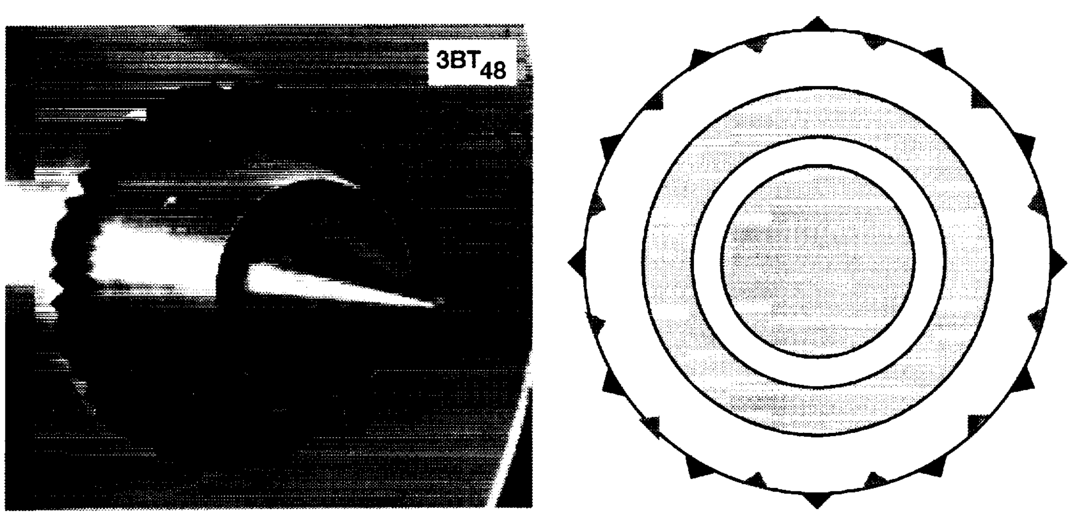

Figure 5.—Tabs on fan nozzle only.

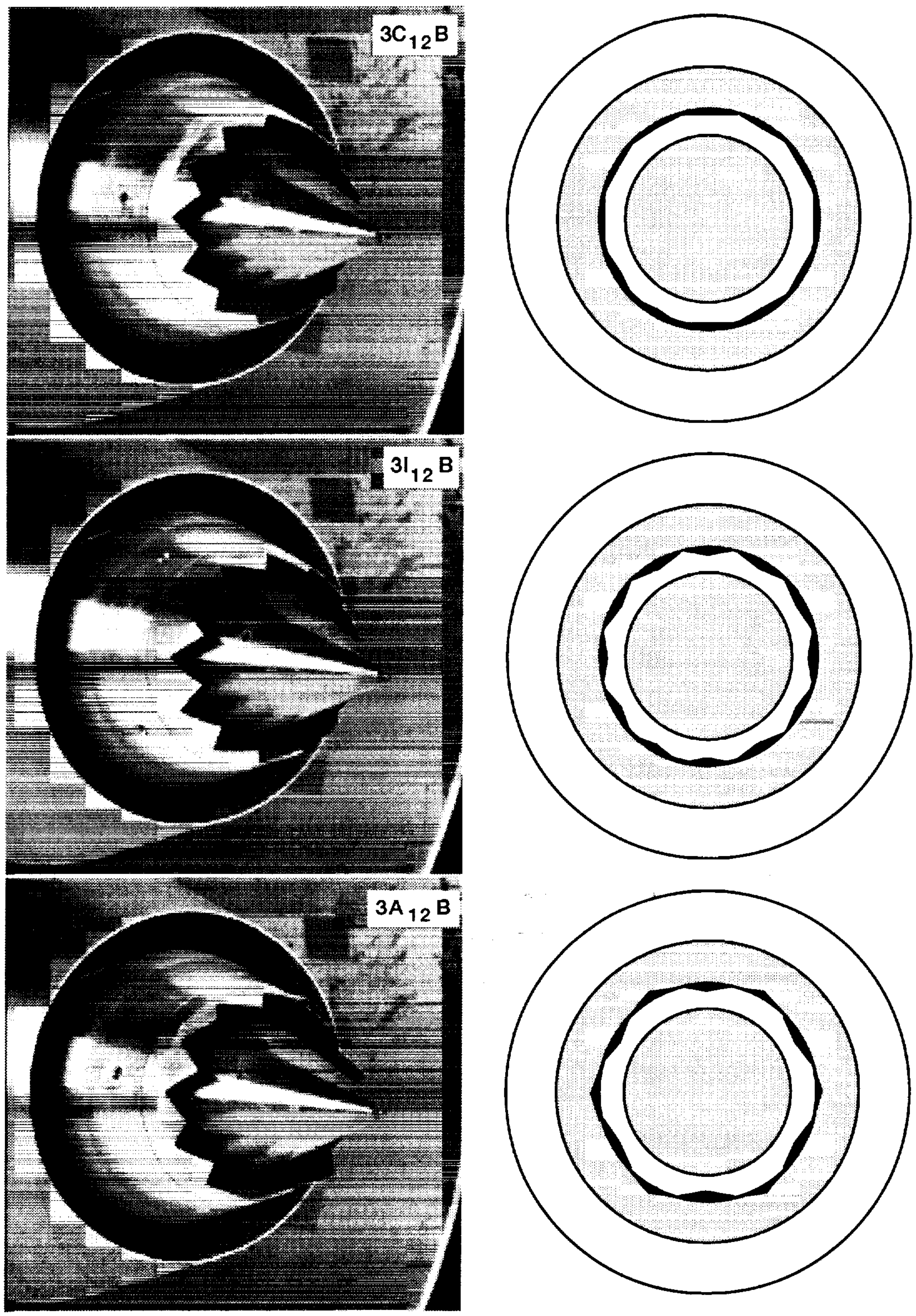

Figure 6.—Chevrons on core nozzle only.

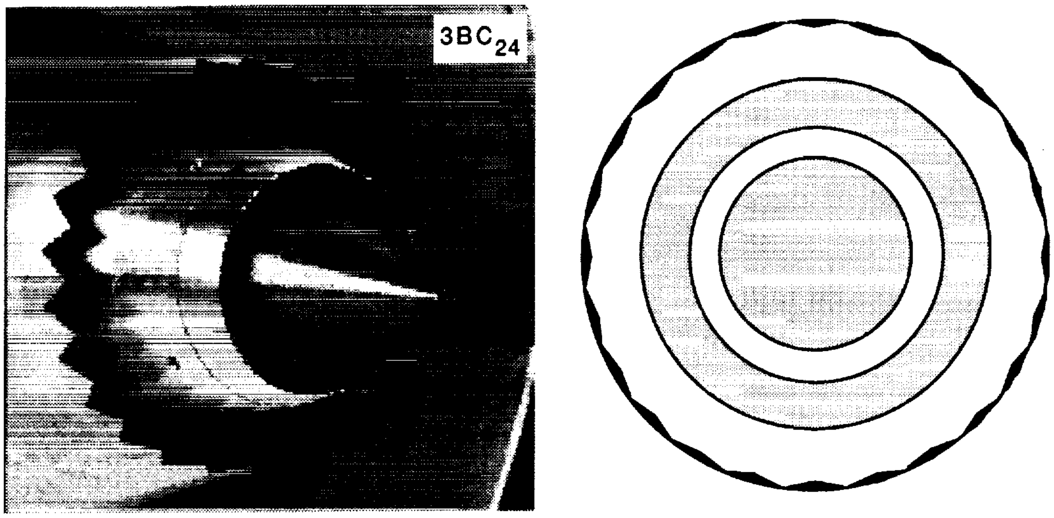

Figure 7.—Chevrons on fan nozzle only.

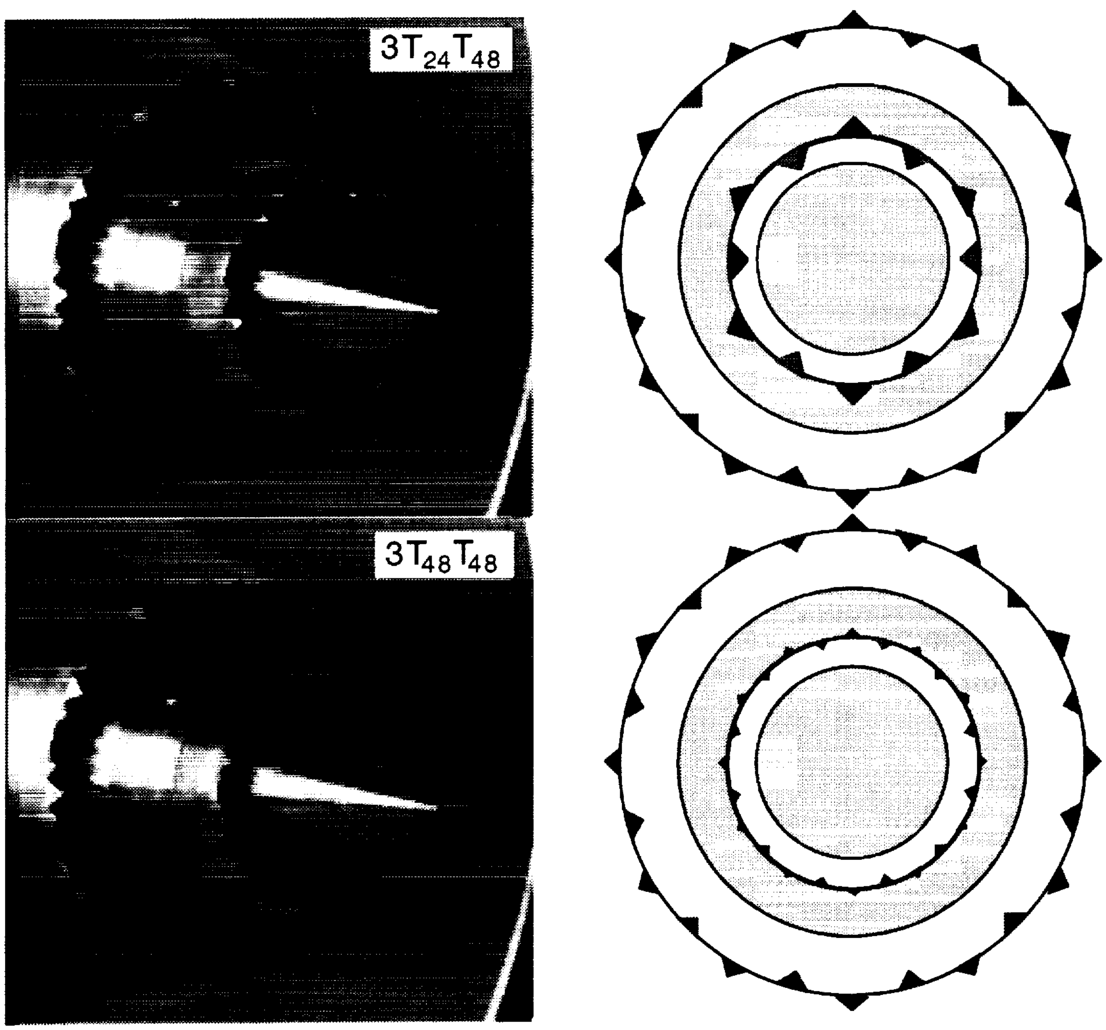

Figure 8.—Core and fan modifications simultaneously.

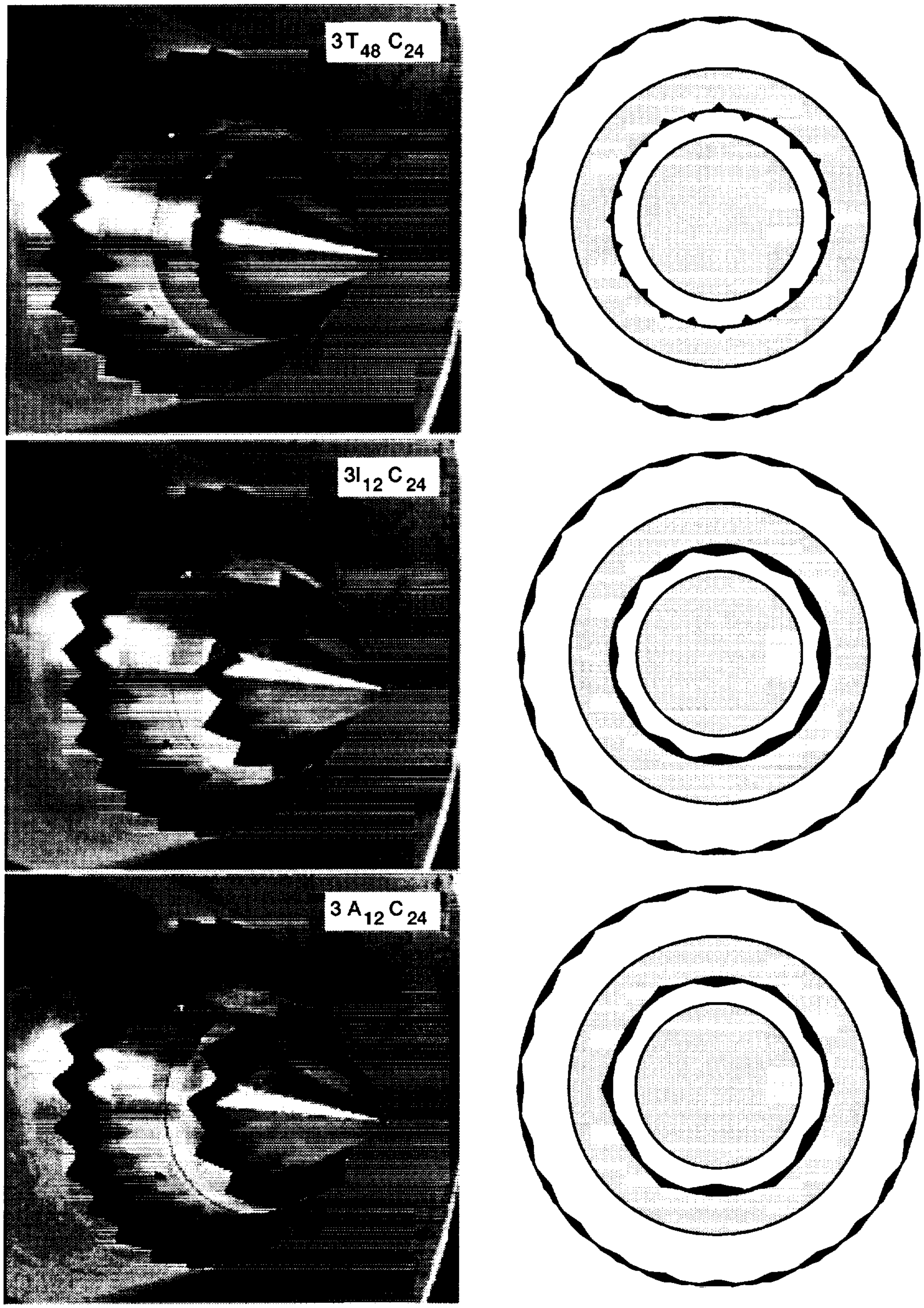

Figure 8.—Continued.

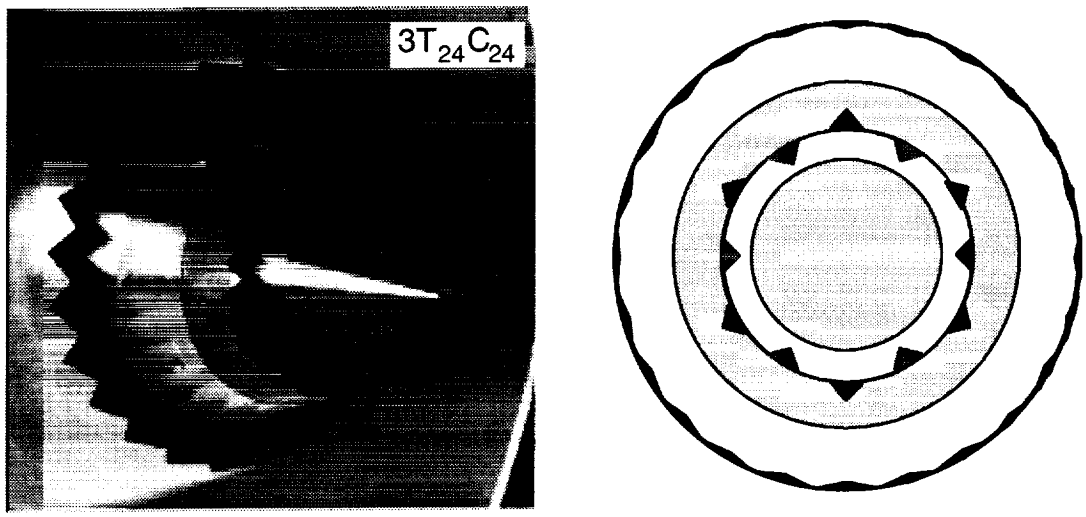

Figure 8.—Concluded.

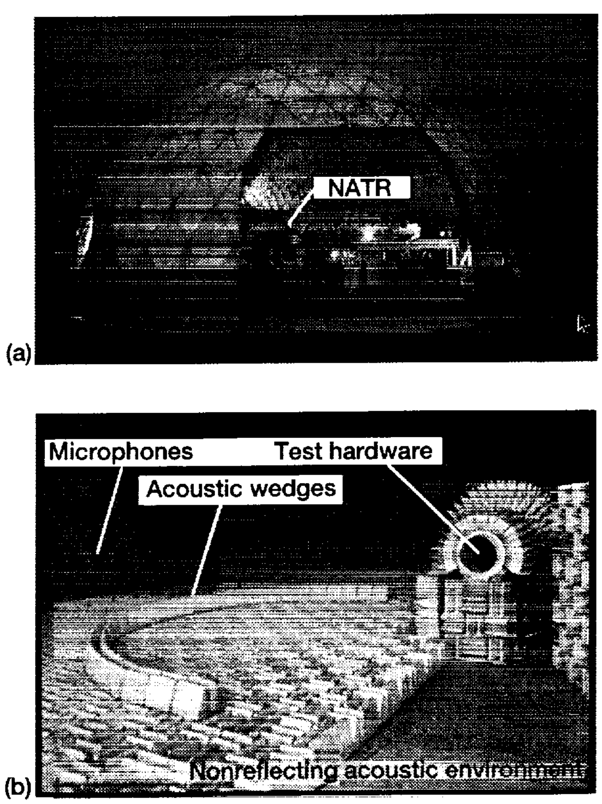

Figure 9.—Aeroacoustic Propulsion Laboratory (AAPL). (a) Outside. (b) Inside.

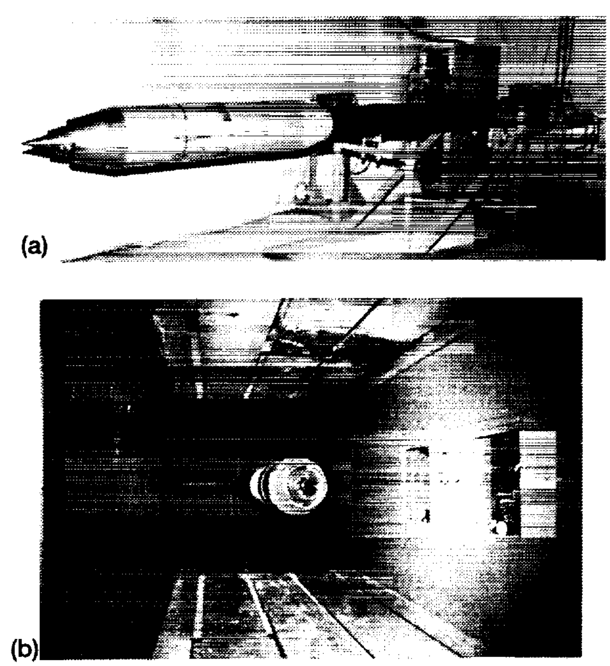

Figure 10.—Thrust stands at Aero Systems Engineering FluiDyne Aerotest Group. (a) Static. (b) Flight.

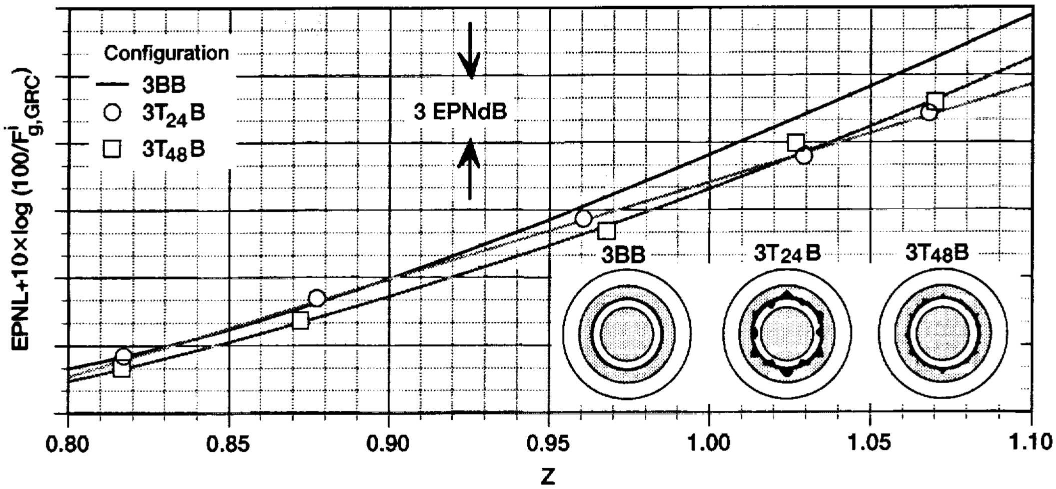

Figure 11.—Effective perceived noise level benefits with tabs on core nozzle.

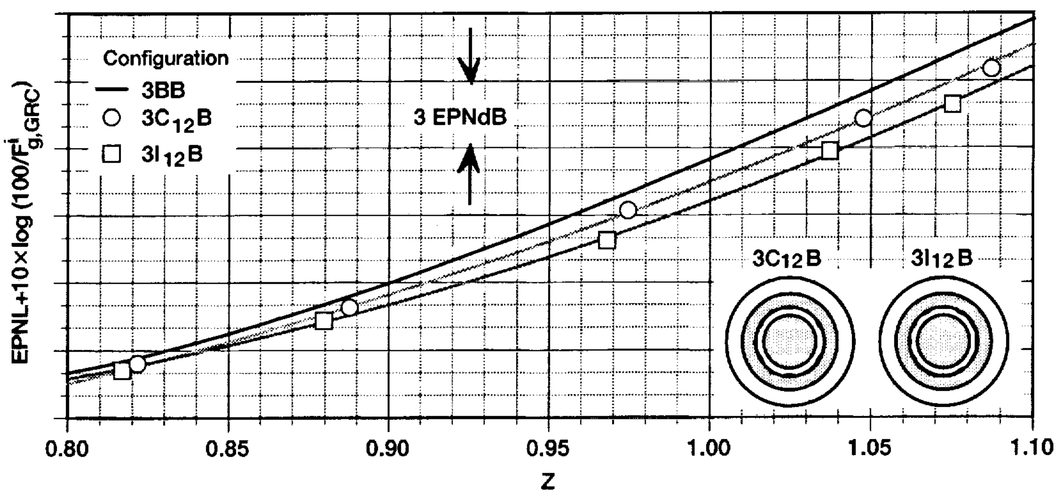

Figure 12.—Effective perceived noise level benefits with chevrons on core nozzle.

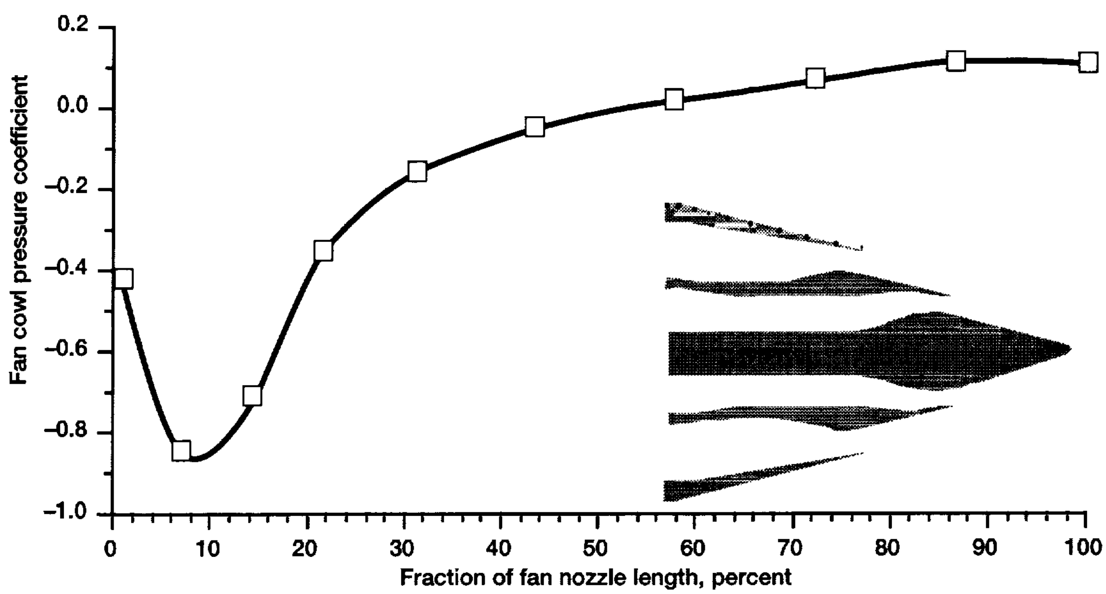

Figure 13.—Static pressure distribution on fan cowl at Mach 0.8.

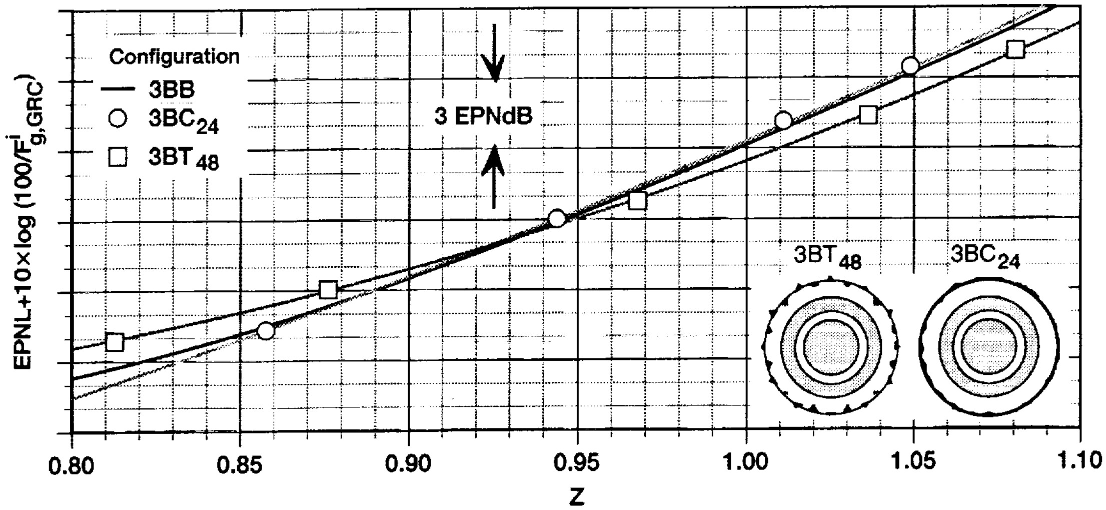

Figure 14.—Effective perceived noise level benefits with tabs and chevrons on fan nozzle.

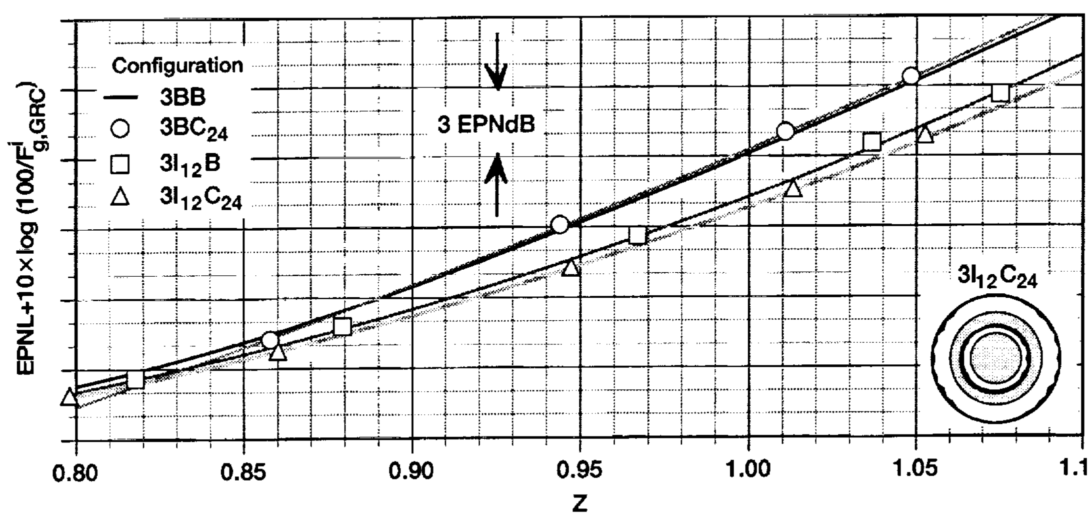

Figure 15.—Effective perceived noise level benefits with chevrons on core and nozzles simultaneously.

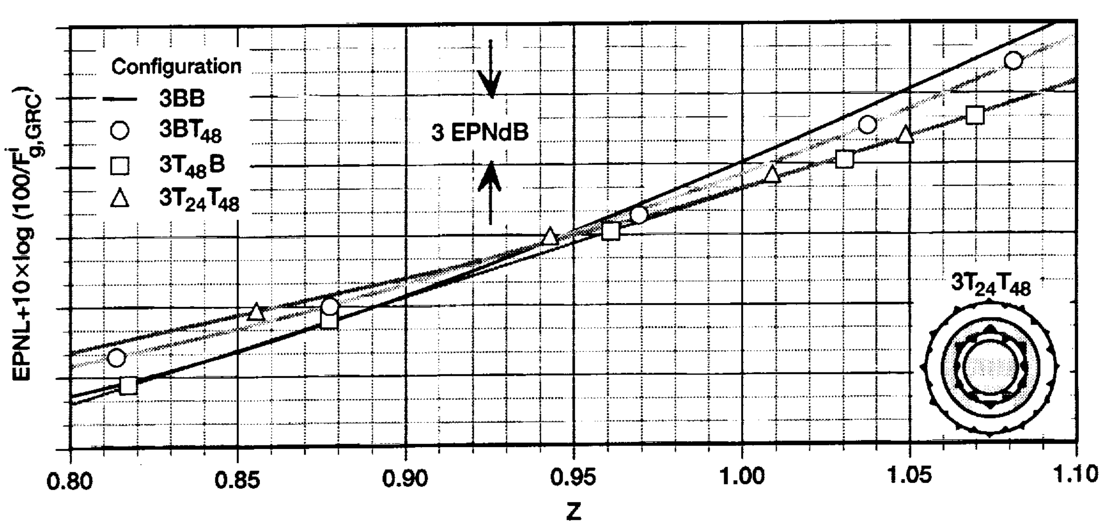

Figure 16.—Effective perceived noise level benefits with tabs on core and nozzles simultaneously.

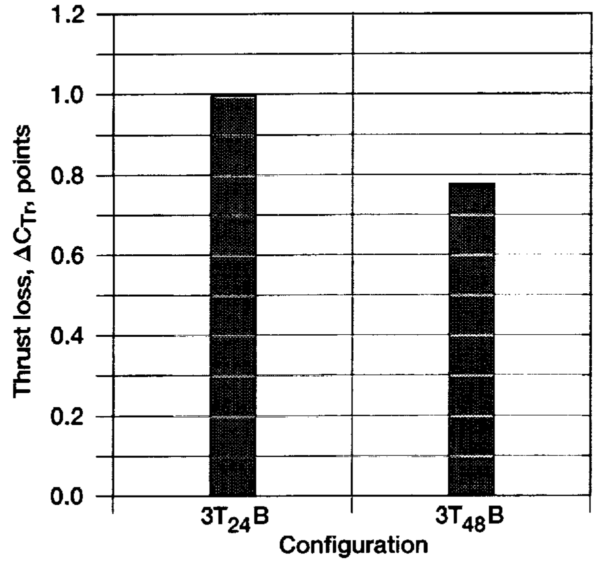

Figure 17.—Tabs on core.

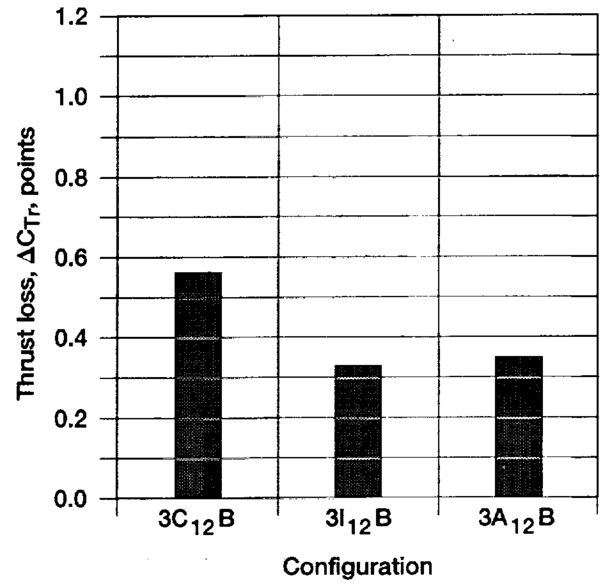

Figure 18.—Chevrons on core.

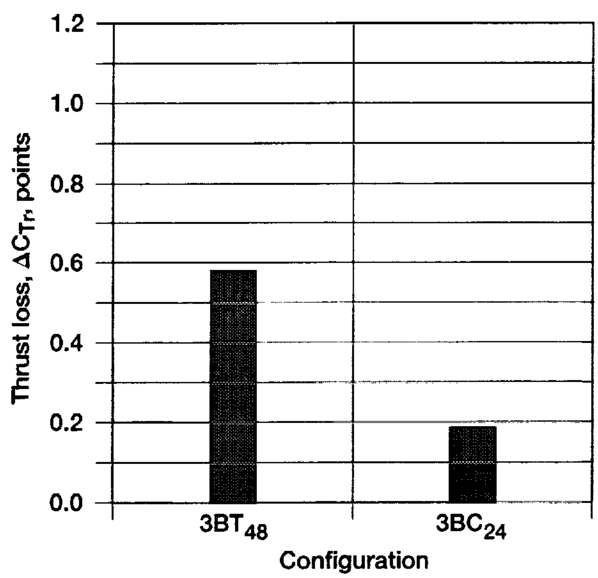

Figure 19.—Tabs and chevron fan.

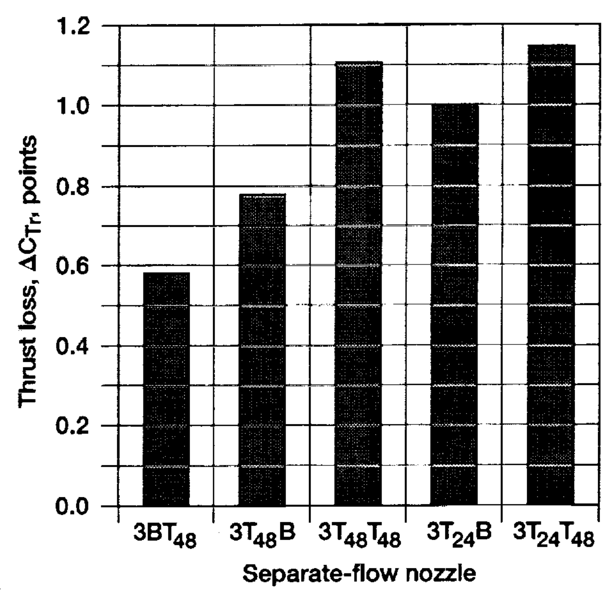

Figure 20.—Tabs on both nozzles.

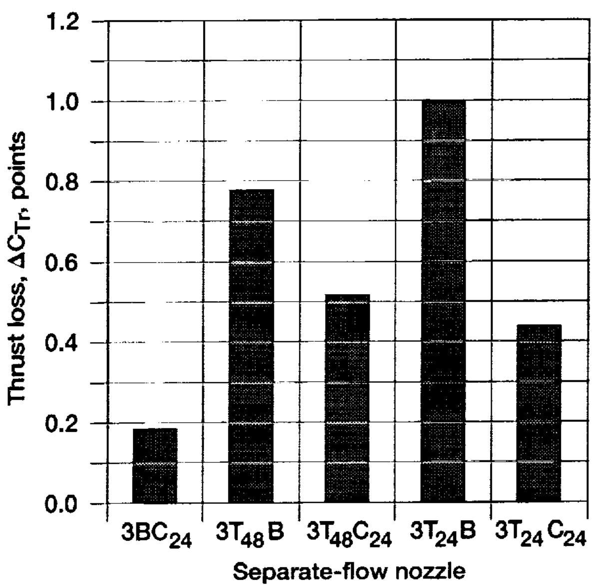

Figure 21.—Tabs with chevrons.

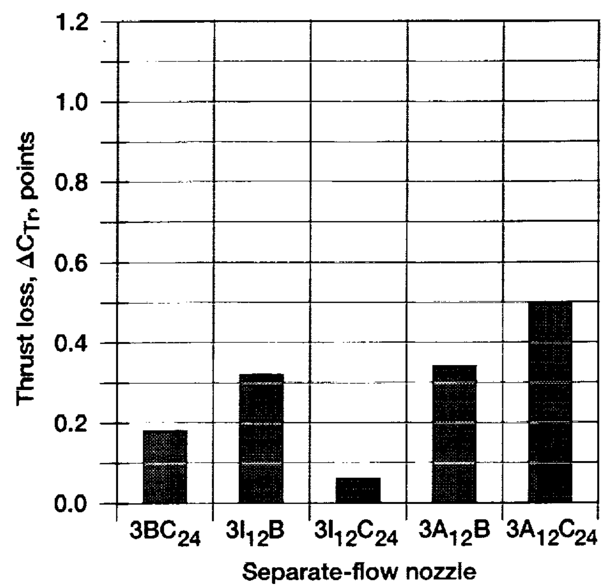

Figure 22.—Chevrons on both nozzles.

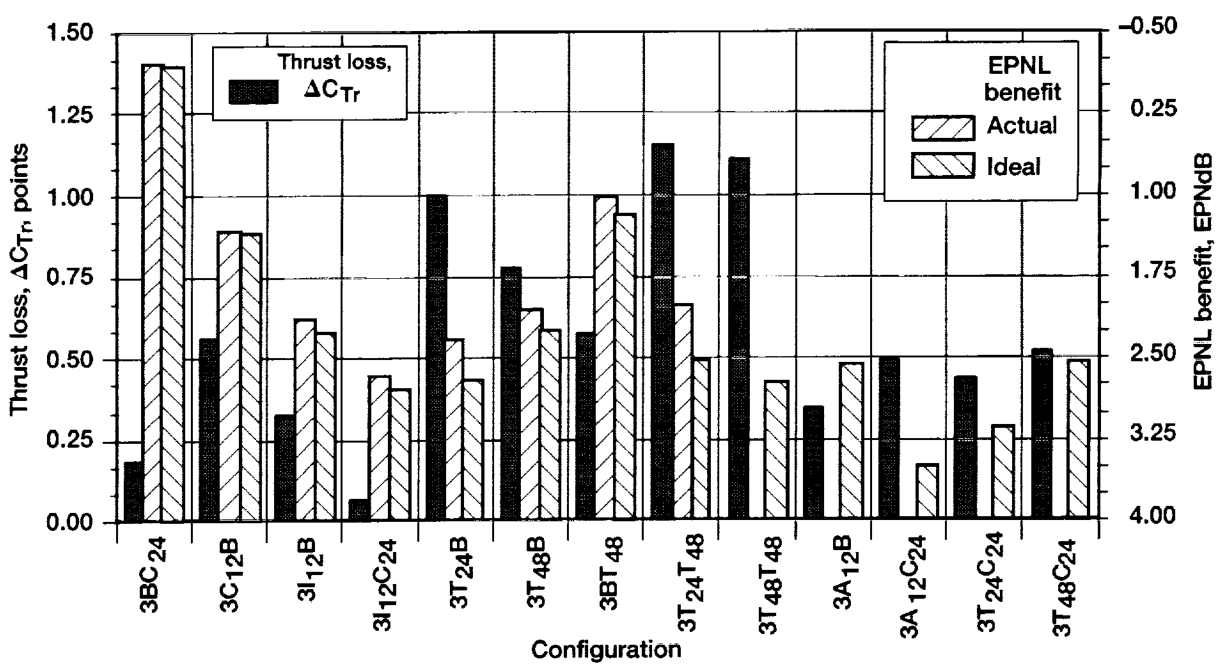

Figure 23.—Effective perceived noise level and cruise thrust losses relative to 3BB.

REPORT DOCUMENTATION PAGE

Form Approved
OMB No. 0704-0188

1. AGENCY USE ONLY (*Leave blank*)	2. REPORT DATE	3. REPORT TYPE AND DATES COVERED
	June 2000	Technical Memorandum

4. TITLE AND SUBTITLE

Acoustics and Thrust of Separate-Flow Exhaust Nozzles With Mixing Devices for High-Bypass-Ratio Engines

5. FUNDING NUMBERS

WU-522-81-11-00

6. AUTHOR(S)

Naseem H. Saiyed, Kevin L. Mikkelsen, and James E. Bridges

7. PERFORMING ORGANIZATION NAME(S) AND ADDRESS(ES)

National Aeronautics and Space Administration
John H. Glenn Research Center at Lewis Field
Cleveland, Ohio 44135-3191

8. PERFORMING ORGANIZATION REPORT NUMBER

E-11714

9. SPONSORING/MONITORING AGENCY NAME(S) AND ADDRESS(ES)

National Aeronautics and Space Administration
Washington, DC 20546-0001

10. SPONSORING/MONITORING AGENCY REPORT NUMBER

NASA TM—2000-209948
AIAA 2000-1961

11. SUPPLEMENTARY NOTES

Prepared for the Sixth Aeroacoustics Conference and Exhibit cosponsored by the American Institute of Aeronautics and Astronautics and Confederation of European Aerospace Societies, Lahaina, Hawaii, June 12-14, 2000. Naseem H. Saiyed and James E. Bridges, NASA Glenn Research Center, and Kevin L. Mikkelsen, Aero Systems Engineering, 358 Fillmore Avenue East, St. Paul, Minnesota 55107. Responsible person, Naseem H. Saiyed, organization code 5940, (216) 433-6736.

12a. DISTRIBUTION/AVAILABILITY STATEMENT

Unclassified - Unlimited
Subject Category: 71 Distribution: Nonstandard

This publication is available from the NASA Center for AeroSpace Information, (301) 621-0390.

12b. DISTRIBUTION CODE

13. ABSTRACT (*Maximum 200 words*)

The NASA Glenn Research Center recently completed an experimental study to reduce the jet noise from modern turbofan engines. The study concentrated on exhaust nozzle designs for high-bypass-ratio engines. These designs modified the core and fan nozzles individually and simultaneously. Several designs provided an ideal jet noise reduction of over 2.5 EPNdB for the effective perceived noise level (EPNL) metric. Noise data, after correcting for takeoff thrust losses, indicated over a 2.0-EPNdB reduction for nine designs. Individually modifying the fan nozzle did not provide attractive EPNL reductions. Designs in which only the core nozzle was modified provided greater EPNL reductions. Designs in which core and fan nozzles were modified simultaneously provided the greatest EPNL reduction. The best nozzle design had a 2.7-EPNdB reduction (corrected for takeoff thrust loss) with a 0.06-point cruise thrust loss. This design simultaneously employed chevrons on the core and fan nozzles. In comparison with chevrons, tabs appeared to be an inefficient method for reducing jet noise. Data trends indicate that the sum of the thrust losses from individually modifying core and fan nozzles did not generally equal the thrust loss from modifying them simultaneously. Flow blockage from tabs did not scale directly with cruise thrust loss and the interaction between fan flow and the core nozzle seemed to strongly affect noise and cruise performance. Finally, the nozzle configuration candidates for full-scale engine demonstrations are identified.

14. SUBJECT TERMS	15. NUMBER OF PAGES	16. PRICE CODE
Jet noise; Turbofan engines; Nozzles; Acoustics	24	A03

17. SECURITY CLASSIFICATION OF REPORT	18. SECURITY CLASSIFICATION OF THIS PAGE	19. SECURITY CLASSIFICATION OF ABSTRACT	20. LIMITATION OF ABSTRACT
Unclassified	Unclassified	Unclassified	